



Strained graphitic carbon nitride for hydrogen purification



S.W. de Silva*, A. Du, W. Senadeera, Y. Gu

School of Chemistry, Physics and Mechanical Engineering Queensland University of Technology, Brisbane 4001, Australia

ARTICLE INFO

Keywords:

Hydrogen purification
Graphitic carbon nitride
Strain tuning
Molecular dynamics
Density functional theory

ABSTRACT

Hydrogen purification from a mixture of gas is a critical step in hydrogen production as an energy source and other clean energy applications. Recently gas purification using membranes with sub-nanometer pores, such as porous graphene has offered an attractive option which purifies the targeted gas from other impurity gases based on size exclusion exploiting the differences in the gases' molecular size. Using a combination of density functional theory (DFT) and molecular dynamic (MD) simulations, we demonstrate that graphitic carbon nitride ($g\text{-C}_3\text{N}_4$), a graphene like 2-dimensional nanomaterial can effectively purify H_2 from CO_2 and CH_4 . However, under neutral conditions the H_2 flux across the membrane is comparatively weak, and our theoretical analysis shows that the flux can be significantly improved by widening the pore area via applying biaxial strains as low as 2.5% and 5% on the membrane. Interestingly, the strain tuning only improves the membranes H_2 permeability, while its excellent H_2/CO_2 and H_2/CH_4 selectivity is not compromised.

1. Introduction

The demand for cleaner energy has incited greater interest in hydrogen energy as it offers a superior alternative to conventional fossil fuel combustion, thanks to its high energy density [1], higher energy conversion efficiency and its environmental friendly nature [2]. Current H_2 production methods include, steam-methane reforming, coal gasification, water-electrolysis etc. [3]. Irrespective of the production method, a critical step common to every method is hydrogen purification step from a mixture of gases.

Among numerous gas separation techniques, membrane separation is regarded superior due to its intrinsic low energy requirements, simple operation [4] and higher tunability. Membrane technology for hydrogen separation exploits the difference in molecular size between hydrogen and other impurity gases. Among various membrane types, such as polymeric [5], inorganic [6–8], and hybrid types [9], graphene and graphene like two dimensional membranes attract greater interest due to their atomic thickness. A membrane's performance is measured by its selectivity and permeability, which normally shows inversely proportional behaviour. However, atomically thin single layer 2D material which has the ultimate thinness, is known to exceed this limitation. Therefore, porous graphene [10–18] and graphene like materials such as graphynes [19,20], graphitic carbon nitrides [21,22] have been explored for gas separation applications.

Two dimensional C_3N_4 is a graphene like carbon nitride material, which has attracted the interest of the scientific community due to its interesting chemical and photocatalytic properties, and excellent

thermal properties [23,24]. It is the most stable of the carbon nitride family, which consists of tri-s-triazine building blocks [25]. Another advantage of this material is its facile synthesis. The common top-down synthesis methods are liquid exfoliation under sonication and thermal exfoliation with the aid of intercalation compounds [26]. As a candidate for gas purification, it intrinsically owns uniformly distributed regular sized pores, unlike in porous graphene where achieving such a feat is challenging. Further, Cao et al. have successfully synthesised and shown that a $g\text{-C}_3\text{N}_4$ incorporated membranes can effectively purify water from ethanol mixtures where the sieving effects were rendered by the $g\text{-C}_3\text{N}_4$ layers [27].

Here we study the use of $g\text{-C}_3\text{N}_4$ for gas separation applications using first principles and molecular dynamic simulation approaches. Our study evaluates the permeability of small gas molecules: H_2 , CO_2 and CH_4 , across a $g\text{-C}_3\text{N}_4$ membrane. The choice of gas molecules is based on the membrane pore area, and the kinetic diameters of the gas molecules. In this study we primarily focus on the possibility of improving the gas permeability of the $g\text{-C}_3\text{N}_4$ membrane, by subjecting it to small biaxial strains. The findings of this study can find applications in H_2 separation from CO_2 and CH_4 , in refinery waste recovery, H_2 purification and pre combustion CO_2 separation.

2. Computational details

In this study, molecular dynamic simulations were used to analyse the H_2 , CO_2 and CH_4 permeation across the membrane, and first principle DFT calculations were used for geometry optimization of $g\text{-C}_3\text{N}_4$.

* Corresponding author.

E-mail address: suchitra.desilva@qut.edu.au (S.W. de Silva).

C_3N_4 and potential energy scan (PES) for H_2 passage under various strained conditions.

All DFT calculations were carried out using DMol3 module in Materials Studio [28,29]. First, the $g-C_3N_4$ supercell was fully relaxed, allowing the relaxation of both atomic positions and the lattice parameters, and for subsequent geometry relaxation under biaxial strain, the strain is added by increasing the fixed unit-cell dimensions by 2.5%, 5% and 7.5% respectively with the atomic positions allowed to relax. The potential energy barrier for the H_2 molecules crossing through a monolayer was simulated by analysing the gas passage through the centre of the pore with a 3×3 $g-C_3N_4$ periodic system based on transition state theory.

The generalized gradient approximation treated by the Perdew-Burke-Ernzerhof exchange correlation [30] with a basis set of all electron double numerical plus polarization (DNP) was used for DFT calculations. The DFT-D method developed by Grimme et al. [31], was used for the long-range van der Waals corrections. For geometry optimization calculations, a 2×2 cell, with a vacuum slab of 10 Å between sheets, was chosen, and the Brillouin zone was sampled by $3 \times 3 \times 1$ k-points using the Monkhorst-Pack scheme [32], while a 3×3 cell with a 20 Å vacuum slab was used with $7 \times 7 \times 1$ k-points for adsorption and PES calculations. The calculations were carried out with a convergence tolerance of 2×10^{-5} Ha for energy, 4×10^{-3} Ha/Å for gradient and 0.005 Å for displacement. The atomic charges were calculated using the Mulliken charge analysis [33].

All MD simulations were performed using the LAMMPS package [34], with a frozen 6×6 monolayer of $g-C_3N_4$ (approximately $\sim 5.5 \times 5.0$ nm) obtained from DFT geometry optimization, placed in the middle of the simulation box, as shown in Fig. 1. Initially 110 gas molecules were placed in one side of the membrane, which behaves as the gas reservoir. The simulation system has periodic boundary conditions applied in xy-directions and reflective boundary conditions in the z-direction, and the height was varied to achieve various feed pressures. Simulations were carried in the NVT ensemble, with Nosé-Hoover thermostat to maintain the system temperature at 298 K. Each simulation was carried out for a total time period of 10 ns with a time-step of 0.4 fs. The Reax potential developed by Mattson et al. for general purpose hydrocarbon parameterization was used to model the interatomic interactions [35].

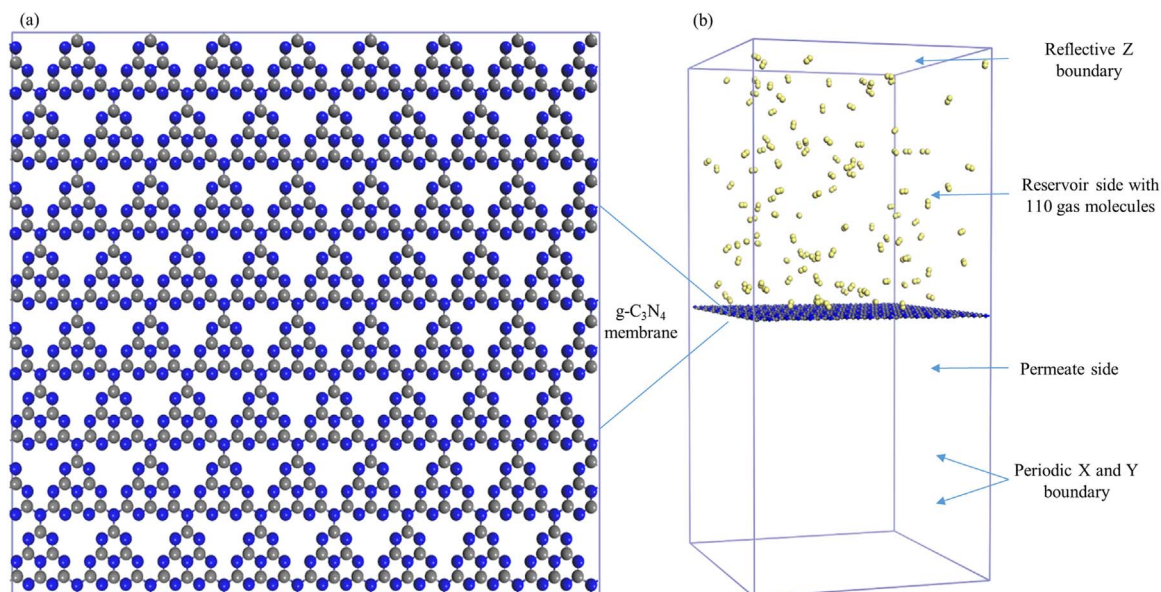


Fig. 1. (a) Top view of the 5×5 nm, $g-C_3N_4$ membrane. (b) Illustration of simulation model. Atom colour code: grey, carbon; blue, nitrogen; yellow, hydrogen. (For interpretation of the references to color in this figure legend, the reader is referred to the web version of this article.)

Table 1
Effect of biaxial strain on $g-C_3N_4$ structure.

Strain		B1	B2	B3	D1	D2
0.0%	Length (Å)	1.48	1.33	1.40	4.77	4.13
	2.5%	1.53	1.35	1.41	4.94	4.28
	Increase %	3.45	1.58	1.00	3.50	3.51
5.0%	Length (Å)	1.57	1.38	1.43	5.08	4.40
	7.5%	1.62	1.41	1.46	5.21	4.51
	Increase %	9.40	5.63	4.66	9.25	9.25

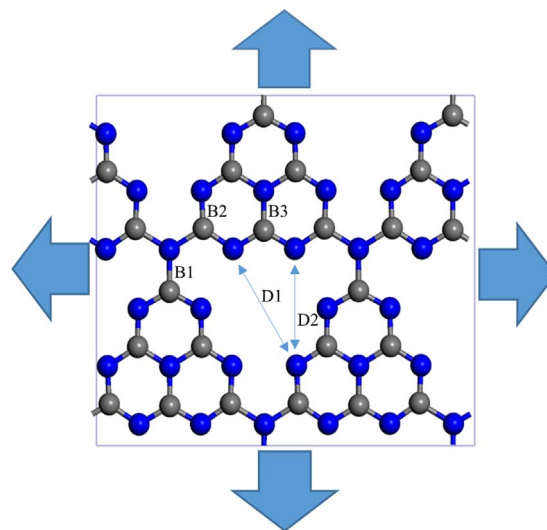


Fig. 2. 2×2 supercell of $g-C_3N_4$. The bonds and distances are labelled. Atom colour code: grey, carbon; blue, nitrogen. (For interpretation of the references to color in this figure legend, the reader is referred to the web version of this article.)

3. Results and discussion

The structural changes induced by applied 2.5%, 5% and 7.5% strain values are summarized and compared against the unstrained cell, in Table 1. The results signify that the change of molecular

Download English Version:

<https://daneshyari.com/en/article/4989162>

Download Persian Version:

<https://daneshyari.com/article/4989162>

[Daneshyari.com](https://daneshyari.com)